Performance assessment of aided GNSS for land navigation

A. Angrisano, antonio.angrisano@uniparthenope.it

S. Gaglione, salvatore.gaglione@uniparthenope.it

C. Gioia, ciro.gioia@uniparthenope.it

Department of Applied Sciences, "Parthenope" University of Naples, Naples Italy

Land navigation includes the methods to determine the time varying position and velocity of a moving object on Earth surface using suitable measurements; it is typically performed in signal-degraded environments where GPS signals are blocked or degraded; hence GPS-only cannot guarantee an accurate and continuous positioning. The multi-constellation approach is a possible way to fill this gap.

In this work GPS/GLONASS systems are combined and single point algorithm performance is assessed for different configurations in urban scenario. GLONASS is nearly fully operational and its inclusion guarantees satellite availability improvement, but the GPS/GLONASS multi-constellation use involves the addition, as further unknown, of the intersystem time-scale offset.

The considered estimation techniques are Least Squares and Kalman Filter. The first method uses only the measurement model, with the drawback of solution unavailability during GNSS outages. The last uses, in addition to a measurement model, a process model allowing the estimation of the unknowns in case of GNSS outage. To improve both methods performances aiding are considered on height and intersystem time scale offset.

The main purposes of this work are the performances assessment of a multi-constellation system relative to GPS-only, adopting the aforesaid estimators, and the benefit evaluation of the aiding.

KEY WORDS

1. Pseudorange 2. GNSS 3. Aiding 4. Kalman Filter

1. INTRODUCTION

GNSS (Global Navigation Satellite Systems) are worldwide, all-weather navigation systems able to provide tridimensional position, velocity and time synchronization to UTC (Universal Time Coordinated) scale [1

,2]. GNSS positioning is based on the reception of signals transmitted by satellites, hence their performances are related to signal quality and operational scenario. GNSS performances are optimal in open sky with many satellites in view and no degraded signal; in these conditions single point position accuracy is about 10 m [2]. Satellite navigation is critical in difficult scenario such as urban canyon and mountainous area, because many GNSS signals are blocked by natural and artificial obstacles or are strongly degraded. Currently GPS (Global Positioning System) is the most widespread GNSS, it is a space-based radio-navigation system developed by the US DoD (Department of Defense) and is fully operative since 1994. In critical environments GPS stand-alone is not able to provide accurate and continuous absolute positioning; a possible approach to solving this problem is to consider the combined use of GPS with other GNSS.

GLONASS (GLObal NAvigation Satellite System) is the Russian alter-ego of GPS and since 2003 it is in modernization phase. GLONASS recent enhancement candidates it as an alternative to GPS, but also as a component of multi-constellation system.

Another element of a multi-constellation system could be the European satellite system Galileo, and the Chinese BeiDou. Waiting for these developing systems, in this research are considered only GPS and GLONASS.

An integrated GNSS system is characterized by a significantly increased satellite availability respect to GPS or GLONASS only, ensuring a positioning improvement in "hostile" environments [3]. The performances of the integrated system are increased in terms of:

- Continuity, directly related to satellite availability,
- Accuracy, enhanced by observation geometry improvement and
- Integrity, because the increased availability improves the detection process of gross errors in the measurements set [4 , 5].

The considered GNSS are very similar but for our purpose a significant difference is their time scale offset; therefore their combined use involves the addition of a further unknown to estimate, i.e. the intersystem time scale offset, which requires the “sacrifice” of one measurement. A possible way to fully use the GPS/GLONASS combination is the employment of a pseudo-measurement, which takes into account the quasi-constancy of this parameter [6]. A further aiding could be adopted considering the altitude slow variations usually experimented in urban navigation.

A purpose of this research is the performance assessment in difficult scenario of different single point GNSS configurations, with specific interest to investigate the benefits of GLONASS inclusion relative to GPS stand-alone.

Different methods can be adopted to estimate the navigation parameters in single point positioning (using pseudorange and Doppler observables); the most common estimators are Least Squares (LS) [7 , 8] and Kalman Filter (KF) [9 , 10].

The LS method is not able to provide navigation unknowns in case of measurement deficiency, while KF guarantees a continuous solution owing to the process model containing equations representing the navigation parameter behaviour.

Different GNSS configurations are analysed and compared in order to assess: the benefits of the GLONASS inclusion relative to GPS only case, the performance of the different estimation techniques (i.e. LS and KF) to process GNSS data. A further goal of this work is the benefit assessments obtained applying constraints on altitude and on time difference between GPS and GLONASS. The performances of the different configurations are analysed in term of RMS and maximum error for horizontal and vertical component, and solution availability.

2. GNSS OVERVIEW

GNSS are worldwide, all-weather navigation systems able to provide tridimensional position, velocity and time synchronization to UTC scale [1 , 2]. GPS and GLONASS are herein the considered GNSS, they are similar for many aspects, such as the operational principle described in the next section, but with some meaningful differences detailed in section 2.2.

2.1. *Operational Principle*

GNSS positioning is based on the one-way ranging technique: the time of travel of a signal transmitted by satellites is measured and scaled by speed of light to obtain the satellite-user distance, used to compute receiver coordinates. The receiver clock offset relative to system time scale must be estimated too. The measured range between receiver and satellite is called pseudorange (PR), whose equation is:

$$\rho = d + c\delta t_u + \varepsilon_\rho \tag{1}$$

where ρ is the PR measurement, d is the geometric distance receiver-satellite, $c\delta t_u$ is the receiver clock offset (scaled by speed of light c) and ε_ρ contains the residual errors after satellite-based and atmospheric error corrections.

Equation (1) holds for both single GNSS (i.e. GPS or GLONASS only) and $c\delta t_u$ is referred to the time scale of the considered system. In multi-constellation case a further unknown, representing the inter-system time offset, must be estimated.

GNSS receivers are also able to provide Doppler measurements, defined as the time derivative of observable phase [1 , 2] and related to the relative motion between receiver and satellites. Doppler observable is directly converted in a pseudorange rate information and its measurement equation is formally similar to (1) [2]:

$$\dot{\rho} = \dot{d} + c\dot{\delta}t_u + \varepsilon_{\dot{\rho}} \tag{2}$$

where $\dot{\rho}$ is the PR rate measurement, $\dot{d}$ is the time derivative of the geometric distance receiver-satellite, $c\dot{\delta}t_u$ is the receiver clock drift (scaled by speed of light c) and $\varepsilon_{\dot{\rho}}$ contains the residual errors after satellite-based corrections.

2.2. *GPS-GLONASS Differences*

GPS and GLONASS are very similar but with some meaningful differences, classifiable as: constellation, signal and reference differences, summarized in Table 1 (and a detailed in [11] [12]).

Table 1. GPS and GLONASS Comparison (adapted by [11])

	Parameter	GPS	GLONASS
Constellation	Number of SV	24 (Expandable)	24
	Orbital Planes	6	3
	Orbital Altitude (Km)	20200	19100
	Orbit Inclination (deg)	55°	64.8°
	Ground Track Period	1 Sidereal Day	8 Sidereal Days
	Layout	Asymmetric	Symmetric
Signal	Carrier Frequencies (MHz)	1575.42 1227.60	1602+K*0.5625 1246+K*0.4375
	Ranging Code Frequencies (MHz)	C/A: 1.023 L2C: 1.023 P: 10.23 M: 10.23	C/A: 0.511 P: 5.11
	Multiple Access Schemes	CDMA	FDMA
	Broadcast Ephemerides	Keplerian	ECEF
Reference	Datum	WGS84	PZ90.02
	Time Scale	GPS Time	GLONASS Time

About the constellations, the nominal number of satellites is 24, but GPS constellation provides for the eventuality of surplus satellites with no pre-defined slots. GLONASS orbits are lower than GPS ones and are more inclined, allowing a better coverage at high latitudes. GLONASS satellites orbital period is shorter than

GPS one, with ground tracks repeating every 8 sidereal days for the first and every day for the second. Moreover the space segment of GLONASS system is a walker constellation, i.e. has a "symmetric" configuration with the slots evenly spaced on each plane and constant argument of latitude displacement between the planes [13]. On the other hand GPS constellation is intentionally "asymmetric": the number of satellites on the planes can be different owing to the surplus satellites and the space vehicles are unevenly distributed on the orbit, in order to optimize the constellation coverage in case of one satellite outage [14].

About the signal, all the GPS satellites broadcast signals at the same carrier frequencies L1 and L2, while each GLONASS satellite uses a different carrier frequency. So GPS and GLONASS systems use different multiple access schemes: respectively CDMA (Code Division Multiple Access, the transmitting satellites are distinguished by the code) and FDMA (Frequency Division Multiple Access, the transmitting satellites are distinguished by the frequency). The next generation of GLONASS satellites (Glonass-K) is planned to implement the CDMA strategy to improve the compatibility with GPS [11].

In addition the chip rate of GLONASS C/A and P codes is about half of the corresponding GPS codes. The chip width - defined as the inverse of the chip rate - is related with the receiver high-frequency error. For typical receivers the standard deviation of this error is about 1/100 of the chip width, corresponding to about 3 m and 0.3 m for GPS C/A and P codes, and to about 6 m and 0.6 m for GLONASS C/A and P codes [14].

Moreover the satellite broadcast ephemerides, stored in the GPS navigation message, are Keplerian parameters and are transformed in ECEF (Earth Centered Earth Fixed) frame using the orbital propagation algorithm [15]; the broadcast ephemerides in GLONASS navigation message are directly expressed in ECEF frame [16] but anyway a propagation algorithm is necessary to compute the satellite position in the desired epoch (usually the epoch of transmission of the signal).

GPS and GLONASS systems adopt different coordinate frames to express the satellite and user coordinates, respectively WGS84 (World Geodetic System 1984) and PZ90 (Parametry Zemli 1990), whose details are in [15 , 16]. The two reference frames are nearly coincident, but a measurement combination from both systems require a seven-parameters transformation; neglecting this transformation yields a position error from a single receiver of metric order [17]. Starting from September 20 2007, an improved version of the GLONASS reference frame is in use, called PZ90.02 [18].

GPS and GLONASS systems adopt different reference time scales, connected with different UTC realizations. In detail GPS time is connected with UTC(USNO), the UTC maintained by US Naval Observatory; UTC scale is occasionally adjusted of one second to keep it close to the mean solar time (connected to the astronomical definition of time). GPS time scale is indeed continuous and so GPS time scale and UTC(USNO) differ for an integer number of seconds (called leap seconds, currently 15 s). Moreover GPS time and UTC(USNO) are maintained by different master clocks, producing a further difference of typically less than 100 ns; this difference is broadcast to the users in the navigation message.

GLONASS time scale is connected to UTC(RU), the UTC as maintained by Russia. GLONASS time is adjusted by leap seconds, according to the UTC adjustments, so they do not differ for an integer number of seconds, but only for a difference less than 1 millisecond, broadcast in the GLONASS navigation message.

The transformation between GPS and GLONASS times is expressed by the following formula [6]:

$$t_{GPS} = t_{GLO} + \tau_r + \tau_u + \tau_g \tag{3}$$

where

$\tau_r = t_{UTC(RU)} - t_{GLO}$ is broadcast in the GLONASS navigation message,

$\tau_u = t_{UTC(USNO)} - t_{UTC(RU)}$ must be estimated and

$\tau_g = t_{GPS} - t_{UTC(USNO)}$ is broadcast in the GPS navigation message.

To perform the transformation (3), the difference between UTC(USNO) and UTC(RU) should be known, but this information is not provided in real-time. This problem is generally solved including the difference between the systems time scales as unknown when GPS and GLONASS measurements are used together.

The GPS-GLONASS system time offset is broadcast via the navigation data as non-immediate parameter included in the GLONASS almanac [16], but does not take into account the inter-system hardware delay bias which is dependent on specific receiver [6].

3. ESTIMATION TECHNIQUES

Estimation is the process of obtaining a set of unknowns (state vector or simply state) from a set of uncertain measurements, according to a definite optimization criterion [19]. To estimate the state, a functional relationship has to be defined with the measurements, usually referred to as the measurement model. The discrete and linear version of such matrix equation is show below:

$$\boldsymbol{z}_k = \boldsymbol{H}_k \boldsymbol{x}_k + \boldsymbol{\eta}_k \tag{4}$$

with $\boldsymbol{z}_k$ measurement vector, $\boldsymbol{H}_k$ frequently referred to as the geometry matrix (and corresponds to the measurement connection matrix), $\boldsymbol{x}_k$ state vector, $\boldsymbol{\eta}_k$ measurement noise vector and the subscript k representing the epoch [14].

The measurement model could be solved for the unknowns if the number of (independent) equations is at least equal to the number of the unknowns. If other equations are included in addition to the measurement model, the set of unknowns can be estimated even in case of measurement lack. These further equations can be obtained considering information about the system state dynamics, usually referred to as process model. The discrete and linear version of process model is show below:

$$\boldsymbol{x}_{k+1} = \boldsymbol{\Phi}_{k+1,k} \boldsymbol{x}_k + \boldsymbol{w}_k \tag{5}$$

where $\boldsymbol{\Phi}_{k+1,k}$ is the transition matrix and $\boldsymbol{w}_k$ is the process noise vector, which takes into account the model uncertainty.

The inclusion of the process model can provide in general a better estimation of the system state vector, if the model represents properly the state behaviour. The estimation methods adopted in this research are the LS method, using only the knowledge of the measurement and the KF using also the process model.

3.1. *Least Squares*

The Least Squares method is the most common estimation procedure in geomatic applications and its estimation process is based purely on the measurements. The LS approach is to obtain a state estimate minimizing the sum of the square residuals, defined as:

$$\boldsymbol{r}_k = \boldsymbol{z}_k - \boldsymbol{H}_k \hat{\boldsymbol{x}}_k \tag{6}$$

LS solution and the associated covariance matrix are:

$$\begin{aligned} \hat{\boldsymbol{x}}_k &= \left(\boldsymbol{H}_k^T \boldsymbol{W} \boldsymbol{H}_k\right)^{-1} \boldsymbol{H}_k^T \boldsymbol{W} \boldsymbol{z}_k \\ \boldsymbol{C}_x &= \left(\boldsymbol{H}_k^T \boldsymbol{W} \boldsymbol{H}_k\right)^{-1} \end{aligned} \tag{7}$$

The weighting matrix $\boldsymbol{W}$ can be set as the inverse of the measurement covariance matrix $\boldsymbol{R}$, weighting the accurate measurements more and the noisy ones less [20]; in this work $\boldsymbol{W}$ is related to a suitable variance model of the observations, depending on satellite elevation, described below:

$$\sigma_{PR}^2 = a + b * 10^{\left(\frac{-el}{10}\right)} \tag{8}$$

where el is the satellite elevation and coefficients a and b must be chosen according to the environment and the user equipment [21]. The coefficients used in this research ($a = 10$ and $b = 20$) were obtained empirically by processing data collected in urban environment. For the pseudorange rate measurements the same function is used, but the value of the coefficients in this case are $a = 4$ and $b = 10$.

3.2. *Kalman Filter*

The Kalman Filter estimation is a technique commonly used in navigational applications, which uses knowledge about measurements and state vector dynamics and so adopts both measurement (4) and process models (5). The measurement model is formally identical to the model used in LS, with the additional assumption of zero-mean white noise with Gaussian distribution for the measurement noise. The KF is a recursive algorithm using a series of prediction and update steps to obtain an optimal state vector estimate in a minimum variance sense [9 , 10].

The prediction step, used to predict the state vector and the associated covariance matrix from the current to the next epoch, is based on the assumed process model:

$$\begin{aligned} \widehat{\boldsymbol{x}}_{k+1}^{-} &= \boldsymbol{\Phi}_{k+1,k}\widehat{\boldsymbol{x}}_{k}^{+} \\ \boldsymbol{P}_{k+1}^{-} &= \boldsymbol{\Phi}_{k+1,k}\boldsymbol{P}_{k}^{+}\boldsymbol{\Phi}_{k+1,k}^{T} + \boldsymbol{Q}_{k} \end{aligned} \tag{9}$$

where the superscript "-" indicates a predicted (or a priori) quantity (i.e. before the measurement update) and the superscript "+" indicates a corrected (or a posteriori) quantity (i.e. after the measurement update). $\boldsymbol{P}$ is the covariance matrix of the state vector and $\boldsymbol{Q}$ is the covariance matrix of the process noise.

The update step is used to correct the predicted state and covariance matrix with the measurements, as shown below:

$$\begin{aligned} \widehat{\boldsymbol{x}}_{k+1}^{+} &= \widehat{\boldsymbol{x}}_{k+1}^{-} + \boldsymbol{K}_{k+1}\boldsymbol{v}_{k+1} \\ \boldsymbol{P}_{k+1}^{+} &= (\boldsymbol{I} - \boldsymbol{K}_{k+1}\boldsymbol{H}_{k+1})\boldsymbol{P}_{k+1}^{-} \end{aligned} \tag{10}$$

where $\boldsymbol{K}$ is the Kalman gain matrix and $\boldsymbol{v}$ is the innovation vector respectively defined as

$$\begin{aligned} \boldsymbol{K}_{k+1} &= \boldsymbol{P}_{k+1}^{-}\boldsymbol{H}_{k+1}^{T}\left(\boldsymbol{H}_{k+1}\boldsymbol{P}_{k+1}^{-}\boldsymbol{H}_{k+1}^{T} + \boldsymbol{R}_{k+1}\right)^{-1} \\ \boldsymbol{v}_{k+1} &= \boldsymbol{z}_{k+1} - \hat{\boldsymbol{z}}_{k+1} = \boldsymbol{z}_{k+1} - \boldsymbol{H}_{k+1}\widehat{\boldsymbol{x}}_{k+1}^{-} \end{aligned} \tag{11}$$

The innovation vector can be considered as an indication of the amount of information introduced in the system by the current measurements. The Kalman gain matrix is a weighting factor, indicating how much the new information contained in the innovation vector influences the final state vector estimate.

4. IMPLEMENTATION

4.1. *PVT Algorithm*

In this research PVT (Position-Velocity-Time) algorithms (detailed in Fig. 1) are developed in MatLab® environment to process GNSS data in single point mode; the software belongs to a tool implemented at PArthenope Navigation Group (PANG).

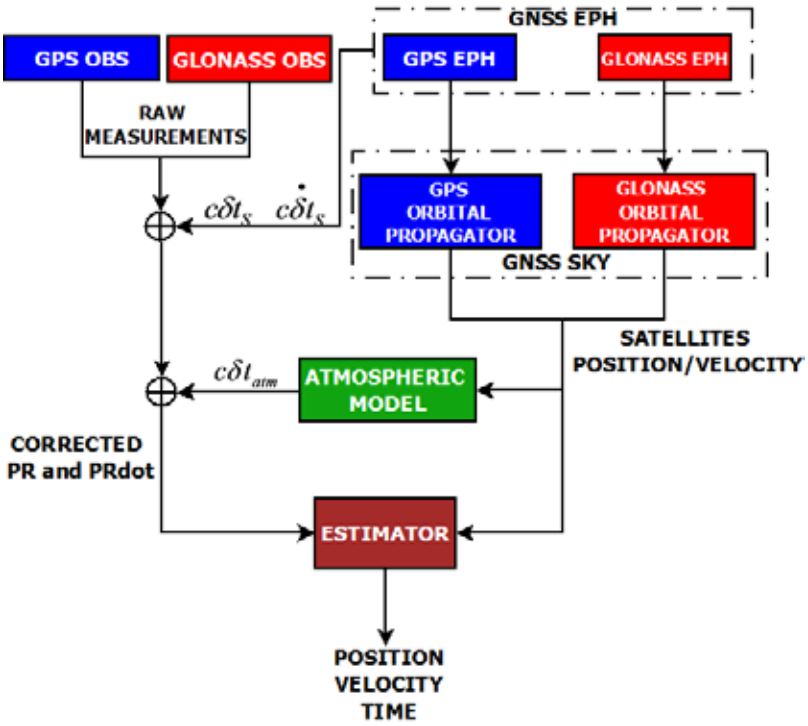

Figure 1. PVT Algorithm Scheme

Main inputs are the GNSS raw measurements - i.e. pseudorange and Doppler - and the GNSS ephemerides, used to compute satellite position and velocity; different orbital propagators are implemented for the considered GNSS because the ephemerides are differently parameterized. The GPS orbital propagator is extensively treated in [14 , 22], while for GLONASS the main reference is [16].

Raw measurements are corrected for satellite clock and atmospheric errors, specifically Klobuchar and Hopfield models are adopted to reduce ionosphere and troposphere delays respectively [23 , 24].

The measurement model consists of equations as (1) and (2), linearized for the unknowns, and assumes the following expression:

$$\boldsymbol{\Delta\rho} = \boldsymbol{H} \cdot \boldsymbol{\Delta x} + \boldsymbol{\varepsilon} \tag{12}$$

where $\boldsymbol{\Delta\rho}$ is the difference between actual and predicted measurements, $\boldsymbol{\varepsilon}$ is the residual error vector, $\boldsymbol{\Delta x}$ is the state vector, detailed below:

$$\boldsymbol{\Delta x} = \begin{bmatrix} \boldsymbol{\Delta P} & \boldsymbol{\Delta V} & \Delta(c\delta t_b) & \Delta(c\delta t_d) & \Delta\left(c\delta t_{sys}\right) \end{bmatrix}^T \tag{13}$$

The state vector contains the receiver position and velocity error used to correct the previous navigation parameter estimation; receiver clock bias ($c\delta t_b$) and drift ($c\delta t_d$) errors; and $c\delta t_{sys}$ is the difference between GPS and GLONASS intersystem time scales error.

Using the local reference frame ENU (East – North – Up), the explicit form of $\boldsymbol{H}$ matrix is:

$$H = \begin{bmatrix} H_{GPS}^{PR} \\ H_{GLO}^{PR} \\ H_{GPS}^{PRdot} \\ H_{GLO}^{PRdot} \end{bmatrix} = \begin{bmatrix} a_E & a_N & a_U & 0 & 0 & 0 & 1 & 0 & 0 \\ a_E & a_N & a_U & 0 & 0 & 0 & 1 & 0 & 1 \\ b_E & b_N & b_U & a_E & a_N & a_U & 0 & 1 & 0 \\ b_E & b_N & b_U & a_E & a_N & a_U & 0 & 1 & 0 \end{bmatrix} \tag{14}$$

where $a_E = \frac{-E_S}{d_0}$, $a_N = \frac{-N_S}{d_0}$, $a_U = \frac{-U_S}{d_0}$ are the direction cosines of the unit vector from the approximate position to the observed satellite, E_S N_S U_S are the satellite coordinates in the considered ENU frame. If the visible satellites belong to the same constellation the design matrix is modified deleting last column, because in single constellation mode it is not possible to estimate the intersystem bias. The coefficients b_E, b_N, b_U, are defined as: $b_E = \frac{\partial P\dot{R}}{\partial E}\Big|_{\underline{\hat{x}}} = \frac{V_{E0}-V_{SE}}{d_0} - \frac{E_S \cdot \dot{d}_0}{d_0^2}$, $b_N = \frac{\partial P\dot{R}}{\partial N}\Big|_{\underline{\hat{x}}} = \frac{V_{N0}-V_{SN}}{d_0} - \frac{N_S \cdot \dot{d}_0}{d_0^2}$, $b_U = \frac{\partial P\dot{R}}{\partial U}\Big|_{\underline{\hat{x}}} = \frac{V_{U0}-V_{SU}}{d_0} - \frac{U_S \cdot \dot{d}_0}{d_0^2}$, V_{SE} V_{SN} V_{SU} are the satellite velocity component expressed in ENU frame, V_{E0} V_{N0} V_{U0} are the previous estimate of receiver velocity components, d_0 is the a priori estimation of the receiver-satellite distance and $\dot{d}_0$ is the a priori estimation of the receiver-satellite relative velocity.

For the KF the linearized measurement model (12) is used with a constant velocity process one; both models are linearized around the most recent estimate of the state vector. In so doing an Extended Kalman Filter (EKF) is implemented where the velocity errors is modelled as a random walk process and $c\delta t_{sys}$ as a random constant process to take into account its quasi-constancy [6]. Thus, the corresponding PVT error dynamic model is:

$$\begin{aligned} \delta\dot{P} &= \delta V \\ \delta\dot{V} &= \eta_v \\ c\dot{\delta t}_b &= c\delta t_d + c\eta_b \\ c\dot{\delta t}_d &= c\eta_d \\ c\dot{\delta t}_{sys} &= \eta_{sys} \end{aligned} \tag{15}$$

where η_v is the process driving white noise with spectral density q_v; η_b is clock error driving white noise with spectral density q_t, η_d is the clock drift driving noise with spectral density q_d, and η_{sys} is the inter system bias driving noise with spectral density q_{sys}.

The velocity error spectral density, q_v, is computed based on typical accelerations experienced in pedestrian navigation [25]. Its horizontal component were set as 1 m/s/√Hz while for the vertical one the value chosen is 0.1 m/s/√Hz . The clock error spectral densities are computed using Allan variance model, a detailed description is in [10 , 25].

Developed PVT algorithms operate in a closed-loop mode, i.e. every epoch the state vector is estimated and is used to correct the nominal state, then the state vector is reset to a null vector [10 , 25]. The strategy is preferred to open-loop, because errors on the estimated navigation parameters are small enough to maintain valid the assumptions for the linearization process.

4.2. *Aiding on Inter-System Time Scale*

If GPS and GLONASS measurements are used together, the difference between the systems time scales must be estimated, limiting a full utilization of the multi-constellation, because one equation is "sacrificed" to estimate the further unknown.

The offset between GPS and GLONASS time scales can be considered constant in a brief interval [6], hence a pseudo-measurement, observing directly $c\delta t_{sys}$, can be introduced as follow:

$$\left(c\delta t_{sys-aid} - c\delta t_{sys0}\right) = [\mathbf{0}_{1\times(n-1)} \quad 1] \cdot \boldsymbol{\Delta x} \tag{16}$$

where

$c\delta t_{sys-aid}$ is an "old" estimation of the parameter, computed with low value of the corresponding state variance/covariance matrix, $c\delta t_{sys0}$ is the previous state element and n is the number of states.

Equation (16) can be included in the measurement model (12), allowing a GPS/GLONASS solution in LS case with 4 mixed visible satellites; this aiding is also used in case of sufficient measurements (≥5 mixed satellites) to enhance measurement model redundancy.

4.3. *Aiding on Altitude*

In urban navigation the height is usually slowly variable during brief time intervals; for this reason a further aiding equation, observing directly the altitude state, can be introduced as shown below:

$$(h_{aid} - h_0) = [\mathbf{0}_{1\times 2} \quad 1 \quad \mathbf{0}_{1\times(n-3)}] \cdot \boldsymbol{\Delta x} \tag{17}$$

where h_{aid} is an "old" estimation of the altitude, computed with low value of the corresponding state variance/covariance matrix or with low VDOP (Vertical Dilution Of Precision) value, h_0 is the previous altitude estimation.

Equation (17) can be included in the measurement model (12), allowing in LS case a GPS only (or GLONASS only) solution with 3 visible satellites or a GPS/GLONASS fix with 4 mixed visible satellites; this aiding is also used in case of sufficient measurements to obtain the solution, enhancing the measurement model redundancy.

If both pseudo-measurements (i.e. aiding on altitude and $c\delta t_{sys}$) are used, it is possible to estimate the state vector in LS case with only 3 mixed GPS/GLONASS visible satellites.

5. TEST

5.1. *Description*

The data collection is a pedestrian test (Figure 2) and was carried out on 24th February 2012 about 12:00 pm in Centro Direzionale of Naples (Italy), typical example of urban canyon; many GNSS signals are blocked by skyscrapers or are strongly degraded for the multipath problems.

Figure 2. Pedestrian Test

The total duration of the test is about 30 minutes with 1 Hz data acquisition rate, the speed varies from 0 to 5 km/h without stops and the total distance travelled is about 2.5 km. The trajectory followed is shown in Fig. 3.

Figure 3. Trajectory (from Google Earth)

5.2. *Equipment*

The used receiver is a NovAtel FlexPak-G2 belonging to the OEMV family, a device able to provide single frequency (L1) GPS/GLONASS positioning with 14 channels (setup used is 10 channel dedicated to GPS and 4 for GLONASS); the connected antenna is an Antcom Active L1/L2. The used devices are showed in Fig. 4.

Figure 4. Equipment

5.3. *Reference*

A topographical approach is used for generating a reference solution, specifically the considered trajectory to travel is a polygonal, whose vertexes are surveyed by a total station (consisting of an electronic theodolite integrated with a distance meter). In Fig. 5 the vertexes surveyed and the total station position are marked (the distance between the station and the farthest vertex is about 120 m). Using range and angular measurements the vertex positions relative to the total station are computed; to frame the coordinates in an absolute reference system, two GPS geodetic receivers are placed in the area (indicated as Base 1 and 2 in Fig. 5, Base 1 being coincident with total station, the direction Base1-Base 2 is also used as reference for the angular measurements). To associate an epoch to each surveyed vertex, the rover receiver is equipped with an external device (a button) used to mark the transit on the vertexes. Finally the points between adjacent vertexes are obtained by linear interpolation considering constant velocity in each segment. The position accuracy of the surveyed vertexes is of centimeter order.

Figure 5. Reference Solution Generation

6. RESULTS AND ANALYSIS

In this research several GNSS configurations are considered and analysed, differing each other for used satellite system, for adopted estimation method and for applied aiding.

The baseline configurations are:

- GPS only with LS (GPS LS),
- GPS/GLONASS with LS (GG LS),
- GPS only with KF (GPS KF),
- GPS/GLONASS with KF (GG KF).

The GLONASS only configuration is not considered due to receiver channel limitation that does not provide redundant measurements.

The aided configurations could include pseudo-measurements on the altitude (indicated with "H" at the end of the corresponding baseline name), on the inter-system time offset (indicated with "T") or both (indicated with "HT").

Pseudorange and Doppler observations are processed in single point positioning. The comparison is carried out in terms of solution availability (i.e. the percentage of time mission when solution is available) and position accuracy; for a fair comparison, accuracy analysis is performed when the solution is obtainable for all configurations (i.e. if GPS LS fix is available) with good geometry (PDOP - Position Dilution Of Precision - less than 10).

6.1. *Baseline Configurations*

The comparison among the baseline configurations in terms of solution availability is summarized in table 2 showing that GLONASS measurement inclusion provides an enhancement of about 5% relative to GPS only adopting LS estimator. KF solutions are continuous, hence they have a 100% of solution availability.

The accuracy analysis is carried out in terms of RMS (Root Mean Square) and maximum errors on position and is summarized in Table 3.

Table 2. Solution Availability of Baseline Configurations

Solution Availability			
GPS LS	**GG LS**	**GPS KF**	**GG KF**
0.79	**0.84**	**1**	**1**

Table 3. Position Accuracy of Baseline Configurations

Configurations	**RMS (m)**		**Max (m)**	
	Horizontal	***Up***	***Horizontal***	***Up***
GPS LS	**7,7**	**5,7**	**47,2**	**32,2**
GG LS	**6,8**	**4,7**	**39,0**	**29,5**
GPS KF	**6,0**	**4,5**	**37,5**	**26,5**
GG KF	**6,0**	**4,2**	**37,1**	**26,4**

In LS case the GPS/GLONASS configuration demonstrates improved performance with respect to GPS only (comparison between line 1 and line 2 of the Table 3), whereas for the KF case the enhancement is less evident (comparison between line 3 and line 4 of the Table 3). The KF configurations guarantee performance

improvements in all considered parameters with respect to LS homologous configurations; the most obvious improvements are on vertical error, because the adopted process model is consistent with the slow altitude variations, typical of land navigation. The horizontal and vertical errors are shown in Fig. 6.

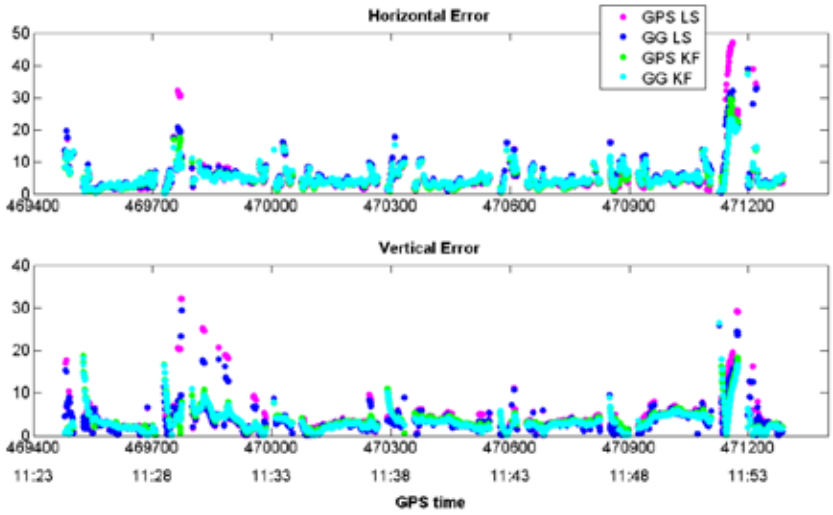

Figure 6. Horizontal and vertical errors of baseline configurations

6.2. *Aided LS Configurations*

The use of the pseudo-measurements - introduced in sections 4.2 and 4.3 - affects the solution availability of LS configurations, allowing a GPS fix with only three visible satellites (aid on altitude) or a GPS/GLONASS fix with only four (aid on altitude or on $c\delta t_{sys}$) or three mixed visible satellites (both aids).

The solution availability enhancement brought by the altitude pseudo-measurements is evident in Table 4, with increment of 7 and 4 % for respectively GPS and GPS/GLONASS case.

In Table 5 the RMS and maximum errors of baseline and altitude aided LS configurations are summarized and the error behaviours are plotted in Fig. 7.

+

Table 4. Solution Availability of Altitude Aided LS Configurations

Solution Availability			
GPS LS	**GPS LS H**	**GG LS**	**GG LS H**
0.79	**0.86**	**0.84**	**0.88**

Table 5. Position Accuracy of Altitude Aided LS Configurations

Configurations	RMS (m)		Max (m)	
	Horizontal	*Up*	*Horizontal*	*Up*
GPS LS	7,7	5,7	47,2	32,2
GPS LS H	5,3	3,4	30,7	7,1
GG LS	6,8	4,7	39,0	29,5
GG LS H	5,6	3,2	31,0	6,8

The use of the altitude aid improves significantly the performances in terms of both RMS and maximum position errors and such enhancements are clear for both GPS only and GPS/GLONASS cases. As expected the vertical component of the solution mainly takes advantage of the aiding. The benefits on the horizontal component can be explained considering that the pseudo-measurement observes directly the altitude, practically constraining it and allowing the actual measurements to estimate mainly the other states; of course if a blunder is present on a measurement, it will strongly affect the horizontal estimation.

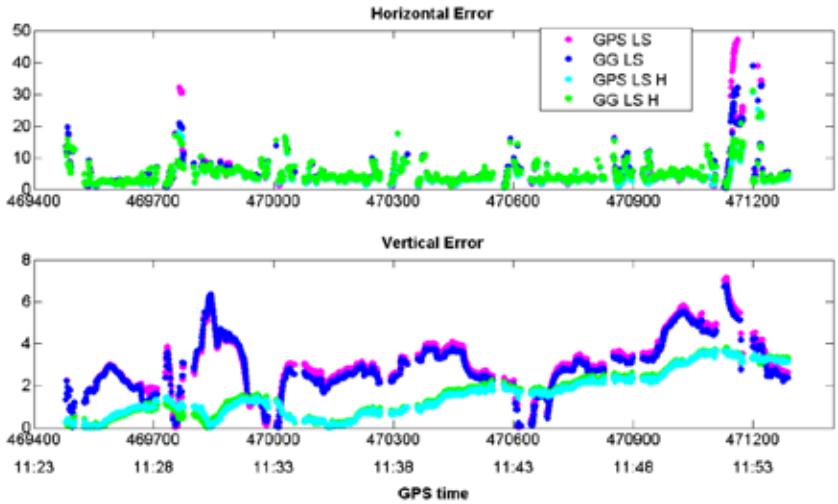

Figure 7. Horizontal and vertical errors of altitude aided LS configurations

The results obtained applying the pseudo-measurement on $c\delta t_{sys}$ to baseline and altitude aided LS configurations are shown in Tables 6 and 7.

Table 6. Solution Availability of $c\delta t_{sys}$ Aided LS Configurations

Solution Availability			
GG LS	GG LS T	GG LS H	GG LS HT
0.84	0.86	0.88	0.89

It is evident that the use of such aid does not help significantly the estimation process, i.e. there is no benefit in terms of position accuracy (from Table 7 comparing line 1 and 2, and line 3 and 4), while it is notable its effect on solution availability (Table 6), which becomes almost 90% when also the altitude aid is used.

Table 7. Position Accuracy of $c\delta t_{sys}$ Aided LS Configurations

Configurations	RMS (m)		Max (m)	
	Horizontal	*Up*	*Horizontal*	*Up*
GG LS	6,8	4,7	39,0	29,5
GG LS T	6,8	4,7	39,0	29,5
GG LS H	5,6	3,2	31,0	6,8
GG LS HT	5,6	3,2	31,0	6,8

6.3. *Aided KF Configurations*

In Table 8, the baseline GPS and GPS/GLONASS KF configurations are compared with aided KF configurations in terms of RMS and maximum errors (the solution availability is unnecessary owing to the continuity of KF solutions). Relative performances are shown in Fig. 8.

Table 8. Position Accuracy of KF Configurations

Configurations	RMS (m)		Max (m)	
	Horizontal	*Up*	*Horizontal*	*Up*
GPS KF	6,0	4,5	37,5	26,5
GPS KF H	5,3	1,9	30,3	3,8
GG KF	6,0	4,2	37,1	26,4
GG KF H	5,5	1,9	30,3	3,7
GG KF T	6,1	4,2	37,2	26,4
GG KF HT	5,7	1,9	30,9	3,7

The use of altitude aid reduces significantly both RMS and maximum errors; the enhancements are clear for both GPS and combined GPS/GLONASS cases and are most significant for the vertical component.

The pseudo-measurement on $c\delta t_{sys}$ does not provide improvements with respect to the baseline configurations; because the process model properly represent the dynamic of the $c\delta t_{sys}$.

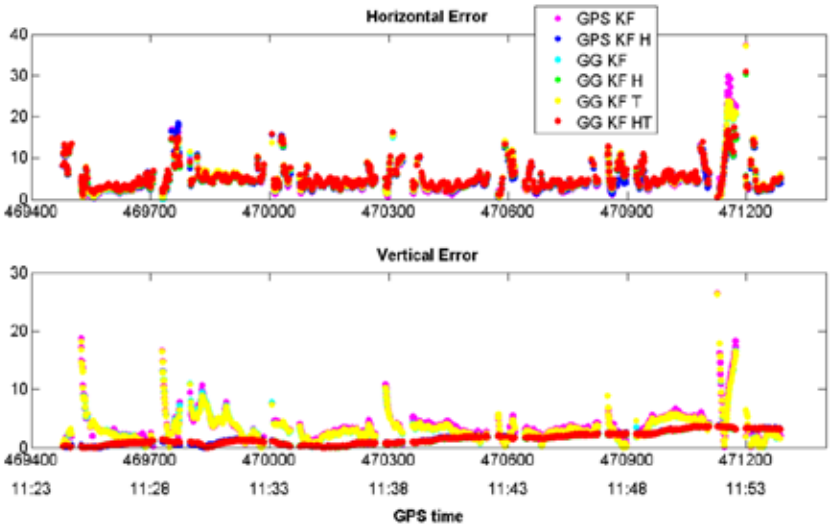

Figure 8. Horizontal and vertical errors of KF configurations

The use of the both aids improves the performances in terms of RMS and maximum errors respect to the baseline configuration, but does not improve the performances with respect to the configuration with only altitude aid.

6.4. *LS vs KF*

The analysis carried out in the previous sections, comparing different GNSS configurations, demonstrated the significant improvements obtained combining GPS and GLONASS measurements and applying an altitude constraint; hence in this section a comparison between GPS and GPS/GLONASS altitude aided configurations is carried out, processing the measurements with LS and KF algorithms, and the performances are shown in Fig. 9. The results obtained with the constraint on the inter-system bias are not considered in this section because it was proved to be ineffective for the tested data. The comparison is in term of RMS and maximum error on the position, the result are summarized in Table 8.

Table 8. Position Accuracy of best LS and KF Configurations

Configurations	RMS (m)		Max (m)	
	Horizontal	*Up*	*Horizontal*	*Up*
GPS LS H	5,3	3,4	30,7	7,1
GG LS H	5,6	3,2	31,0	6,8
GPS KF H	5,3	1,9	30,3	3,8
GG KF H	5,5	1,9	30,3	3,7

For the horizontal component all the configurations guarantee similar performance as shown in Table 9. However the slight degradation of GG configurations is due to the larger errors of GLONASS measurements

relative to GPS ones [26]. For the vertical component the KF estimation shows better results than LS case. With the altitude aid applied the inclusion of GLONASS measurements improves only the solution availability of LS case.

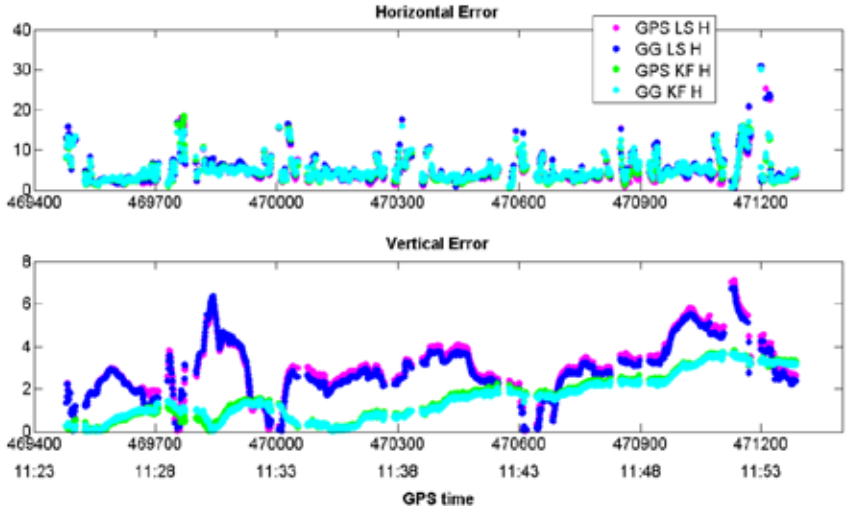

Figure 9. Horizontal and vertical errors of best LS and KF configurations

7. CONCLUSIONS

The main focus of this research is the study of the GNSS performances in single point positioning in urban scenario.

To this purpose different GNSS configurations are analysed and compared in order to assess: the benefits of the GLONASS inclusion relative to GPS only case, the performance of LS and KF to process GNSS data, the improvements obtained applying constraints on altitude and on time difference between GPS and GLONASS.

Based on the results obtained in this paper, GPS/GLONASS configurations show evident improvements with respect to GPS only in terms of solution availability and accuracy, usually considered critical parameters in urban navigation.

The multi-constellation approach need the estimation of a further unknown, i.e. the offset between the systems time scales; the aid on this state avoids the “sacrifice” of one observation, allowing the positioning with 4 mixed visible satellites. The configurations aided in this sense show improvements only in terms of solution availability.

The comparison between the considered estimation methods show that KF solutions demonstrate better performance with respect to LS homologous configurations in terms of RMS and maximum errors and obviously solution availability; the main benefit concerns the vertical component, because the process model adopted is suitable for land navigation.

The altitude aid provides significant improvements in terms of solution availability (for LS) and errors; as expected the vertical components mainly takes advantages of such aiding, but also the horizontal component shows enhancements.

8. FUTURE WORK

The results obtained demonstrate the benefit of the GPS/GLONASS combination with respect to GPS only case; with this in mind a future development of this research will include the Galileo system.

It will be also developed an adaptive KF for vehicular navigation and a suitable RAIM (Receiver autonomous integrity monitoring) technique for urban environment.

The performance assessment of low cost high sensitivity receivers will be a further phase of this work.

REFERENCES

[1] Hoffmann-Wellenhof, B., Lichtenegger, H. and Collins, J., 1992. Global Positioning System: Theory and Practice. Springer New York.

[2] Kaplan, E.D. and Hegarty, J., 2006. Fundamentals of Satellite Navigation. Kaplan, E.D. ed., Understanding GPS: Principles and Applications (second edition), Artech House Mobile Communications Series.

[3] Angrisano, A., Gaglione, S., Gioia, C., 2012. Performance assessment of GPSGLONASS single point positioning in an urban environment. In Press Acta Geodaetica et Geophysica Hungarica

[4] Angrisano, A., Petovello, M.G. and Pugliano, G., 2010. GNSS/INS Integration in Vehicular Urban Navigation. Proceedings of GNSS10 (Portland, OR, 21-24 Sep), The Institute of Navigation.

[5] Angrisano, A., Petovello, M., Pugliano, G., 2012. Benefits of Combined GPS/GLONASS with Low-Cost MEMS IMUs for Vehicular Urban Navigation. Sensors. 2012; 12(4):5134-5158.

[6] Cai, C. and Gao, Y., 2009. A Combined GPS/GLONASS Navigation Algorithm for use with Limited Satellite Visibility, Journal of Navigation (2009), 62: 671-685 Cambridge University Press.

[7] Mikhail, E. M., 1976. Observations and Least Squares. Harper & Row.

[8] Wells, D.E. and Krakiwsky, E. J., 1971. The Methods of Least Squares. Lecture Notes No 18, Department of Surveying Engineering, University of Brunswick.

[9] Kalman, R.E., 1960. A new approach to linear filtering and prediction problems Trans. ASME J. Basic Engr. 35-45 March 1960, 82, pp. 34-45.

[10] Brown, R. G. and Hwang, P.Y.C., 1997. Introduction to Random Signals and Applied Kalman Filtering. John Wiley & Sons.

[11] Cai, C., 2009. Precise Point Positioning Using Dual-Frequency GPS and GLONASS Measurements. MSc Thesis, Department of Geomatics Engineering, University of Calgary, Canada, UCGE Report No. 20291, 2009.

[12] Angrisano, A., 2010. GNSS/INS Integration Methods. PhD Thesis, "Parthenope" University of Naples.

[13] Lucarelli, G., Picone, R., Troisi, S.: 'The loci of satellite positions: a constellation design approach', Celestial Mechanics and Dynamical Astr, 0923-2958 Springer Netherlands, 1998

[14] Parkinson, B. and Spilker, J. J. Jr., 1996. Global Positioning System: Theory And Applications, volume 1, American Institute of Aeronautics and Astronautics, Inc., Washington D.C., USA.

[15] IS-GPS-200. Navstar GPS Space Segment/Navigation User Interfaces, Revision D, ARINC Research Corporation, El Segundo, CA, 2004.

[16] ICD-GLONASS. Global Navigation Satellite System GLONASS Interface Control Document, version 5.1, Moscow, 2008.

[17] Misra, P., Pratt, M. and Burke, B., 1998. Augmentation of GPS/LAAS with GLONASS: Performance Assessment, ION GPS-98, 11th International Technical Meeting of the Satellite Division of the Institute of Navigation.

[18] Revnivykh, S.G. . GLONASS Status, Development and Application, International Committee on Global Navigation Satellite System (ICG) Second meeting, September 4-7, 2007, Bangalore, India, 2007.

[19] Bar-Shalom, Y., Li , X. and Kirubarajan T. Estimation with Applications to Tracking and Navigation, John Willey and Sons, New York, 2001.

[20] Brogan, W. L., 1981. Improvements and Extensions of GDOP Concept for Selecting Navigation Measurements, Final Report for period 1 May 1980 - May 1981 of Nebraska University Lincoln Department of Electrical Engineering.

[21] Kuusniemi, H:. User-Level Reliability and Quality Monitoring in Satellite-Based Personal Navigation, PhD Thesis, Publication 544, Tampere University of Technology, Finland, 2005.

[22] Remondi, B. W.: Computing Satellite Velocity Using the Broadcast Ephemeris, GPS Solutions, 8(3):pp.181-183, 2004.

[23] Klobuchar, J. A.: 'Ionospheric time-delay algorithm for single-frequency GPS users', IEEE Trans. Aerosp. Electron. Syst., 1987, AES-23, (3), pp. 325–331

[24] Hopfield, H. S.: Two-Quartic Tropospheric Refractivity Profile for Correcting Satellite Data, *J. Geophys. Res.*, *74*(18), 4487–4499, doi:10.1029/JC074i018p04487, 1969.

[25] Godha, S.: Performance Evaluation of Low Cost MEMS-Based IMU Integrated With GPS for Land Vehicle Navigation Application, MSc Thesis, Department of Geomatics Engineering, University of Calgary, Canada, UCGE Report No. 20239, 2006.

[26] Angrisano, A., Gaglione, S., Pugliano, G., Robustelli, R., Santamaria, R., Vultaggio, M.: 'A stochastic sigma model for GLONASS satellite pseudorange', Appl. Geomat., 2011, 3, pp. 49–57